**Biogeosciences
Discussions**

BGD

6, 8661–8690, 2009

**Seasonal leaf
dynamics in tropical
grasslands**

P. Choler et al.

Title Page	
Abstract	Introduction
Conclusions	References
Tables	Figures
◄◄	►►
◄	►
Back	Close
Full Screen / Esc	
Printer-friendly Version	
Interactive Discussion	

A simple ecohydrological model captures essentials of seasonal leaf dynamics in semi-arid tropical grasslands

P. Choler[1,2], W. Sea[1], P. Briggs[1], M. Raupach[1], and R. Leuning[1]

[1]CSIRO Marine and Atmospheric Research, P.O. Box 3023, Canberra, ACT, 2601, Australia
[2]Laboratoire d'Ecologie Alpine, UMR CNRS-UJF 5553, Université J. Fourier, Grenoble I, BP53, 38041 Grenoble, France

Correspondence to: P. Choler (philippe.choler@ujf-grenoble.fr)

Abstract

Modelling leaf phenology in water-controlled ecosystems remains a difficult task because of high spatial and temporal variability in the interaction of plant growth and soil moisture. Here, we move beyond widely used linear models to examine the performance of low-dimensional, nonlinear ecohydrological models that couple the dynamics of plant cover and soil moisture. The study area encompasses $400\,000\,\mathrm{km}^2$ of semi-arid perennial tropical grasslands, dominated by C_4 grasses, in the Northern Territory and Queensland (Australia). We prepared 8 yr time series (2001–2008) of climatic variables and estimates of fractional vegetation cover derived from MODIS Normalized Difference Vegetation Index (NDVI) for 400 randomly chosen sites, of which 25% were used for model calibration and 75% for model validation.

We found that the mean absolute error of linear and nonlinear models did not markedly differ. However, nonlinear models presented key advantages: (1) they exhibited far less systematic error than their linear counterparts; (2) their error magnitude was consistent throughout a precipitation gradient while the performance of linear models deteriorated at the driest sites, and (3) they better captured the sharp transitions in leaf cover that are observed under high seasonality of precipitation. Our results showed that low-dimensional models including feedbacks between soil water balance and plant growth adequately predict leaf dynamics in semi-arid perennial grasslands. Because these models attempt to capture fundamental ecohydrological processes, they should be the favoured approach for prognostic models of phenology.

1 Introduction

Most recent advances in empirical models of leaf phenology, i.e. the time dependence of Leaf Area Index (LAI), have been made for temperate deciduous forests where temperature is the main controlling factor (Chuine, 2000). By contrast, leaf phenology in water-limited ecosystems remains poorly captured by current broad empirical ap-

proaches (Botta et al., 2000). Yet, water is the main controlling factor of ecosystem functioning for more than 50% of the land mass (Churkina and Running, 1998; Huxman et al., 2004). Two main reasons may explain these difficulties. First, soil water balance, which has long been recognized as a key driver of plant growth in water-
5 limited ecosystems (Walker and Langridge, 1996; Farrar et al., 1994), is highly variable at the landscape scale and hence difficult to predict in global models. Spatial variability in precipitation and large-scale modelling of runoff and drainage are among difficulties encountered. By contrast, mean air temperature exhibits smoother variations along broad latitudinal or elevation gradients. Second, there are immediate and important
10 feedbacks of plant growth on soil moisture content through water extraction by roots during transpiration. Contrary to temperature, water is a depletable resource exploited by plants at a rate dependent on both resource (soil water availability) and leaf biomass. This leads to nonlinear dynamics of the Lotka-Volterra type (Raupach, 2007) and calls for the development of nonlinear models of interacting soil moisture and vegetation
15 growth. This was highlighted in several conceptual papers in the emerging field of eco-hydrology (Rodriguez-Iturbe et al., 2001; Daly and Porporato, 2005). So far, however, there has been no attempt to evaluate the performance of these nonlinear approaches using long data records of climate and remotely-sensed vegetation greenness.

Long time series of remotely-sensed data of phenology provide opportunities to re-
20 late vegetation cover or greeness with climatic controls (Pettorelli et al., 2005; Daly and Porporato, 2005). A large number of regional (Ji and Peters, 2004; Farrar et al., 1994; Richard and Poccard, 1998) and global (Potter and Brooks, 1998; Lotsch et al., 2003) studies have examined the response of greenness to rainfall or estimates of soil moisture. Most of these studies used linear modelling, with model performance usually
25 maximised by smoothing or lagging the predictors, usually rainfall time series. Though these modelling approaches have proven to be efficient, they do not make explicit the processes linking precipitation, soil moisture dynamics, and water use by plants to sustain growth.

The motivation of the present study is to examine whether low-dimensional, nonlin-

Seasonal leaf dynamics in tropical grasslands

P. Choler et al.

Printer-friendly Version

Interactive Discussion

Full Screen / Esc

ear models outperform their linear counterparts for predicting leaf phenology in water-limited ecosystems. Our philosophy for nonlinear modelling is to capture plant-soil moisture coupled dynamics, while keeping the model tractable and comparable in complexity with a linear model that typically uses 3–5 parameters. This constraint in the number of parameters obviously leads to simplifications for soil water balance and plant growth. However, our purpose is to seek a simple, transparent and portable model that can be used with readily available large-scale climatic and remotely-sensed data and that will enable its inclusion in global land surface models.

In this paper, we used MODIS NDVI time series of the Australian semi-arid Mitchell grasslands as a case study. This choice was motivated by three main factors. First, these grasslands are known to exhibit a rapid response to precipitation (Christie, 1981). Second, phenology is driven by growth of one life-form, i.e. perennial grasses, which removes the problem of differentiating tree and grass contributions to the NDVI signature (Archibald and Scholes, 2007). Third, these grasslands are distributed along a precipitation gradient in northern Australia, offering the opportunity to examine the ability of a single set of parameters to predict leaf dynamics under contrasting precipitation regimes. Our study has three steps: (i) calibrating linear and nonlinear models using time series of climate and NDVI-derived vegetation cover for 400 randomly chosen sites within the Mitchell grasslands; (ii) examining the ability of these models to capture the dynamics of test data sets of vegetation cover; and finally (iii) comparing the performance of these models to predict yearly integrated values of vegetation cover.

2 Material and methods

2.1 Study area

The study area of approximately 400 000 km^2 corresponds to the Mitchell Grass Downs ecoregion (Bailey, 2004), extending from central Northern Territory to central southern

Queensland, Australia (Fig. 1). The lack of trees has been attributed to cracking clay soils and fire prior to European settlement (Orr, 1975). The grasslands are dominated by C_4 perennial grasses, among which Mitchell grass (*Astrebla* spp.), feather-top wire grass (*Aristida* spp.) and Blue grass (*Dichanthium* spp.) are the commonest. These
5 grasslands support an extensive pastoral industry, and shifts in species composition and vegetation cover in response to sheep or cattle grazing have been documented (Orr, 1980a; Foran and Bastin, 1984). The climate is predominantly tropical semi-arid and exhibits a large north-south rainfall gradient. Annual rainfall is associated with pronounced wet-dry seasonality in the north that diminishes in amount and season-
10 ality towards the southeast (Fig. 1). Maximum temperatures remain high throughout the year, though winter (July) minima are significantly lower in southern Queensland compared with the Northern Territory (Fig. 1).

Four hundred sites were randomly chosen within the area of Mitchell grasslands, as given in the digital map of Australia's Native Major Vegetation Subgroups (Aus-
15 tralian Government, Department of the Environment, Water, Heritage and the Arts, (http://www.environment.gov.au/erin/nvis/mvg/)). To avoid potential edge effects, we removed 0.05 degree cells that were directly adjacent to another vegetation sub-group, usually Eucalypt open woodlands. Vegetation physiognomy for all sampled points was further checked using Ikonos images available on Google Earth version
20 4.3 (http://earth.google.com/). Changes in cover of perennial grasses are likely to occur around cattle watering points due to overgrazing and these areas are likely to exhibit anomalous remotely sensed vegetation indices (Pickup et al., 1998). We obtained the location of permanent and semi permanent sources of stock water (bores and dams) from Geoscience Australia's Geodta Topo 250 K vector product
25 (http://www.ga.gov.au/mapspecs/250k100k/). These data were used *a posteriori* to test for a potential effect of the distance to the nearest watering point on model performance.

2.2 Datasets

We used MODIS reflectance data (MOD09A2 Collection 5) from the Oak Ridge National Laboratory Distributed Active Archive Center MODIS website (http://daac.ornl.gov/MODIS/modis.html). The period analysed was from the beginning of July 2000 to
5 end of June 2008 for a total of 368 periods of 8 days each (except for the last period of each year where the period was shorter). We used MOD09 reflectance values in the Red and Near InfraRed to calculate the Normalized Difference Vegetation Index NDVI. Reflectances were averaged over a 2×2 km area around the target point. We tested different areas (4, 16 and 25 km^2) and found no significant effect on the analysis
10 described below. Pixel values that did not have the highest quality flag value were discarded. Missing values were interpolated using a two order polynomial fitting method.

Numerous studies have shown that NDVI can be used as a proxy for green vegetation fraction, V (Myneni et al., 1995; Carlson and Ripley, 1997). Following Carlson et al. (1995), we normalized the NDVI values to estimate V as follow:

15 $$V = [(\text{NDVI}_{obs} - \text{NDVI}_0)/(\text{NDVI}_\infty - \text{NDVI}_0)]^\gamma \qquad (1)$$

where NDVI_{obs} is the observed pixel value, NDVI_0 is that for bare soil and NDVI_∞ is that for full vegetation cover. Different values for γ have been used in previous studies: $\gamma=1$ in a linear mixing model (Gutman and Ignatov, 1998) or $\gamma=2$ as in (Choudhury et al., 1994; Seaquist et al., 2003). There was no qualitative change in the relative
20 performance of the models when γ was varied between these two values and results below are given for $\gamma=2$. Averaged NDVI values during the dry season (July) were used to estimated NDVI_0 for each soil type as soil properties may affect reflectances (Montandon and Small, 2008). A value of 0.75 was assigned for NDVI_∞, corresponding to the averaged maximum NDVI observed during the wet season in the most productive
25 North-Western Mitchell grasslands (near the Gulf of Carpentaria). This value is very similar to those reported for other grasslands (Seaquist et al., 2003).

Before modelling, time series of V were filtered to suppress unusually high or low values. We applied a Savitzky-Golay filter where the original data value V at t_i is

Full Screen / Esc

Printer-friendly Version

Interactive Discussion

replaced by the value of a quadratic polynomial fitted for $2n+1$ points (Savitzky and Golay, 1964), with n being the number of time steps preceding or following t_i. We used a moving window of length $n=2$.

Daily time-series of precipitation (P) and Priestley-Taylor potential evapotranspiration (E) (Priestley and Taylor, 1972) were retrieved from the 0.05 degree resolution SILO database (Australian Government, Bureau of Meteorology http://www.bom.gov.au/silo/). 8-d cumulative sum of P and E matching MODIS time periods were prepared for each site. Details on evapotranspiration estimates are given in Raupach et al. (2008). Gridded data were produced by spatial interpolation of ground-based observations as described in Jeffrey et al. (2001). This dataset is useful for capturing the regional-scale and broad inter-annual patterns of climate variability, but it is of more limited use at finer scales, e.g. rainfall patterns of individual events. For the sampled area, the nearest weather station or rain gauge did not exceed 30 km for 80% of the sites.

Soil data were obtained from the Atlas of Australian Soils (McKenzie et al., 2000; McKenzie and Hook, 1992). The dominant soil type in the Mitchell grassland ecoregion is cracking clay soil. Most of the eastern and northern sites are deep cracking grey soils, coded Ug5.2 and hereafter named "grey soils", while the south-western sites in Queensland exhibit brown-red clay soils, coded Ug5.32 and hereafter named "brown-red soils". Maps for saturated soil water content (W_{sat}) and soil depth (Z) given in McKenzie et al. (2000) were used to calculate a common mean value of 450 mm for soil available water capacity (W_{cap}). We did not have enough data to to differentiate both soil types on the basis of their W_{cap}.

2.3 Modelling approach

We compared two classes of low-dimensional models, hereafter M1 and M2, with the aim of predicting 8-yr long time series of soil water content (W in mm) and vegetation cover (V dimensionless). In the linear model M1, soil water content affects leaf growth but there is no feedback between leaf dynamics and soil water content. This model is

Seasonal leaf dynamics in tropical grasslands

P. Choler et al.

Full Screen / Esc

Printer-friendly Version

Interactive Discussion

given by:

$$(M1) \quad \begin{cases} W_{t+1} = W_t + P_t - \alpha_1 \left(\dfrac{W_t}{W_{cap}}\right) E_t \\ V_{t+1} = V_t + \alpha_2 \left(We_{t-L} - We_{t-L-1}\right) \end{cases} \qquad (2)$$

subject to

(i) $W_{t=0} = W_0; V_{t=0} = V_0$
(ii) $W_{t+1} = \max(0, \min(W_{cap}, W_t))$
(iii) $We_t = \max(0, W_t - \alpha_3)$
(iv) $V_{t+1} = \max(V_{min}, \min(K, V_t))$.

Soil moisture content is calculated using a one-layer bucket model with precipitation
5 (P) as input, and evaporation from bare soil plus plant transpiration (E_t) and run-off
as outputs. Water loss is a function of E_t, relative soil water content (W_t/W_{cap}) and
an exponential decay parameter α_1. Initial values of V and W at $t=0$ are specified
by condition (i). Soil moisture content W is allowed to vary in the interval [0, W_{cap}]
while all precipitation runs off when W reaches W_{cap} (condition ii). We_t is soil water
10 that can be extracted by plant roots and it reaches zero when $W_{t+1}=\alpha_3$ (condition iii).
The parameter α_2 determines the linear sensitivity of V to changes in extractable soil
water content according to a one (M1A) or a two (M1B) parameter ramp function. V
is allowed to vary in the interval [V_{min}, K], where K is the carrying capacity for each
site, estimated as the maximum value of the time series for V at that site (condition iv).
15 Finally, M1 incorporates a lag in the number of time steps (L) to account for a delayed
response of leaf growth to seasonal water availability. L has a considerable effect on
model performance and all analyses were performed with $L=2$ (16 days) since this
consistently gave the best results. Including L adds one more parameter to M1.

The non-linear model M2 includes feedbacks between V and W. This model is written as:

$$(M2) \begin{cases} W_{t+1} = W_t + P_t - \beta_1 (1 - V_t) \left(\frac{W_t}{W_{cap}} \right) E_t - \beta_2 V_t We_t \\ V_{t+1} = \beta_3 \left(\frac{We_t}{W_{cap} - \beta_5} \right) V_t (1 - \frac{V_t}{K}) - \beta_4 V_t \end{cases} \quad (3)$$

subject to

(i) $W_{t=0} = W_0$; $V_{t=0} = V_0$
(ii) $W_{t+1} = \max(0, \min(W_{cap}, W_t))$
(iii) $We_t = \max(0, W_t - \beta_5)$
(iv) $V_{t+1} = \max(V_{min}, \min(K, V_t))$

The two-parameter bucket soil model in Eq. (3) distinguishes bare soil evaporation and plant transpiration. Evaporation from the upper soil layer is modelled as a function of the bare soil fraction $(1 - V_t)$, soil relative water content (W_t/W_{cap}), evaporative demand (E_t) and a parameter β_x. Plant transpiration was modelled as a water-limited process dependent upon the fraction of plant cover (V_t), total amount of extractable water (We_t) and a parameter β_2 that accounts for plant water extraction ability. The dynamics of V is governed by a logistic growth and a mortality term. The growth rate β_3 is modified by the relative amount of extractable soil water content (We_t/W_{cap}) while leaf mortality is a function of V and a decay rate parameter, β_4. A non-zero minimum value of V, V_{min}, is required to ensure leaf growth initiation at the start of the wet season in M2 (see Dickinson et al., 2008 for further discussion). This small amount of persisting above-ground biomass may correspond to near-ground leaf and shoot primordia of perennial grasses. Choosing contrasting V_{min} values did affect parameter estimates in M2, but did not change the goodness-of-fit statistics. Here, we set $V_{min} = 0.001$. For consistency, the same lower limit value for V was used in M1 and M2 although V_{min} had no impact on M1 parameter estimates.

As for M1, we distinguished two cases: M2A does not include a threshold value for the response of transpiration and growth to soil water content, i.e. $\beta_5 = 0$ and $W = We$,

Seasonal leaf dynamics in tropical grasslands

P. Choler et al.

whereas β_5 was a calibrated parameter in M2B. There was no need to include a lag parameter in M2 because the logistic growth model was able to simulate low responsiveness of V to initial increase of W. A similar coupled nonlinear relationship between V and W has been recently proposed by De Michele et al. (2008).

2.4 Model calibration and validation

Parameter estimation was performed using calibrating datasets comprising 100 randomly selected sites. Parameter estimation only relied on the available remotely-sensed data of greenness since we had no soil water content data to add further constraints on parameter estimates. Parameters were optimized using the R package rgenoud (Mebane and Sekhon, 2009). This optimization method combines a genetic algorithm for searching the parameter space and a derivative-based quasi-Newton algorithm developed by Byrd et al. (1995). For difficult convergence problems where multiple local minima may exist, we found this method much more efficient than purely derivative-based methods. The quasi-Newton algorithm allows setting of the lower and upper bounds for a given parameter. This flexibility was required to constrain all parameters to be positive and some to be less than one (β_2 and β_4, see Eq. 3). For each of the 100 calibrated sites, a Coefficient of Variation of the Mean Absolute Error, hereafter CVMAE, was calculated as the Mean Absolute Error (MAE) normalised to the mean of observations (Eq. 4). Willmott et al. (2005) strongly recommended using MAE as the best measure of average error magnitude of a model. This is because goodness-of-fit statistics based on the squaring of an error term, e.g. Mean Square Error (MSE) or Root Mean Square Error (RMSE), are more sensitive to the distribution of errors and often lead to overweighting outliers. Because calibrating sites differ by their mean vegetation cover, MAE naturally tend to increase with increasing mean vegetation cover. We used CVMAE to ensure that each calibrating site had a similar weight on the final estimate of goodness-of-fit. To remove the undesirable influence of outliers, we minimized the median CVMAE value of the 100 training sites, instead of its

mean or its sum. Therefore, the objective function, F, was:

$$F = \text{median}(\text{CVMAE}_1, \ldots, \text{CVMAE}_i, \ldots, \text{CVMAE}_p) \qquad (4)$$

with

$$\text{CVMAE}_i = \text{MAE}_i / \bar{V}_{i,o} = \left(\frac{1}{n} \sum_{t=1}^{n} \left| V_{i,p} - V_{i,o} \right| \right) / \bar{V}_{i,o} \qquad (5)$$

where t is time in periods of 8 d, n is the number of time periods, $p=100$ is the number of calibrating sites, $V_{i,p}$ and $V_{i,o}$ are the predicted and observed values of vegetation cover for site i, respectively, and $\bar{V}_{i,o}$ is the mean vegetation cover of site i. We performed 30 different calibration runs, each conducted with a different subset of 100 sites. The mean values of each parameter resulting from these calibration runs are given in Table 1.

Parameter estimates from each calibration run were used to predict time series of V and W for the remaining 300 testing sites. Several goodness-of-fit statistics were then calculated including R-squared, MSE, CVMSE and their root-mean-square RMSE and CVRMSE, but again MAE and CVMAE were primarily used to assess model performance. On the other hand, the advantage of using the sum of squared errors as goodness-of-fit statistics is that they can be additively partitioned into a systematic and an unsystematic component as described by Willmott (1982). For example, in the case of CVMSE:

$$\text{CVMSE}_{s,i} = \frac{1}{n} \sum_{t=1}^{n} \left(\widehat{V}_{i,p} - V_{i,o} \right)^2 / \bar{V}_{i,o} \qquad (6)$$

$$\text{CVMSE}_{u,i} = \frac{1}{n} \sum_{t=1}^{n} \left(V_{i,p} - \widehat{V}_{i,p} \right)^2 / \bar{V}_{i,o} \qquad (7)$$

with $\widehat{V}_{i,p} = a + b\, V_{i,o}$,

Seasonal leaf dynamics in tropical grasslands

P. Choler et al.

Title Page

Abstract	Introduction
Conclusions	References
Tables	Figures

◀ ▶

◀ ▶

| Back | Close |

Full Screen / Esc

Printer-friendly Version

Interactive Discussion

where a and b are the intercept and slope of the least square regression between the predicted and observed values of V for the calibrating site i, respectively. From Eq. (5), the percentage of systematic error was calculated as $100^*(CVMSE_{s,i}/CVMSE_i)$ and that of unsystematic error as $100^*(CVMSE_{u,i}/CVMSE_i)$. A systematic error approach-
5 ing zero is indicative of a model structure that adequately captures the system dynamics. Using model II regression, or Standardized Major Axis (SMA) regression (Warton et al., 2006), we also tested whether the slope b was significantly different from 1, and the intercept a significantly different from 0.

Finally, we conducted sensitivity analyses by varying one model parameter while
10 keeping the other parameters constant and calculating the relative effect on CVMAE.

Numerical simulations, statistical analyses and all graphics were performed within the R software environment (R Development Core Team, 2007). The source code is available upon request. All computations were performed on the cluster HealthPhy (CIMENT, Université J. Fourier – Grenoble I).

15 **3 Results**

Most of the Mitchell grasslands sites receive between 300 and 400 mm of precipitation during the wet period from November to April (Fig. 2a). For the rest of the year, the median value for rainfall was 48 mm (Fig. 2b). Heavier winter rainfalls occur in the southern part of the studied area (Fig. 1). There was a positive relationship between
20 the maximum vegetation cover K and the mean amount of precipitation during the wet summer period, though there was large scatter around 300–400 mm (Fig. 2a). No such relationship was observed for the dry winter period (Fig. 2b). We did not find any relationship between K and minimum, maximum or mean temperature (data not shown).
25 Table 1 summarizes the calibrated values of the parameters for the four models. Estimates from different calibration runs showed similar variation, i.e. coefficients of variation ranging from 10% to 20%, with the noticeable exception of β_5 for M2B and to

a lesser extent of β_2 for M2A (Table 1). There was a strong discrepancy between M1B and M2B in the estimate of the threshold value for W, with α_3=72 mm and β_5=10 mm. With such a low value for β_5, it is not surprising that the estimates for the other four parameters, from β_1 to β_4, were very similar between M2A and M2B (Table 1).

5   Whatever the goodness-of-fit statistic, the performance of M1A was markedly lower than the three others (Table 2). Conversely, we found no marked contrast in the accuracy of M1B, M2A and M2B (Table 2). MAE and CVMAE of these three models were very similar and MSE and CVMSE were less than 10% higher for M2 models than for M1B (Table 2). The most striking difference between M1B and the two M2 models was

10 in error partitioning. M1B exhibited an inflated systematic error of 55% compared to M2A (31%) or M2B (29%). The higher bias in M1B was due to a consistent underestimation of V (SMA slope of 0.77) (Table 2). Except for M1A, no model had a SMA intercept that differed significantly from 0 (Table 2). Finally, we found only marginal difference between M2A and M2B and chose to keep the simplest one, i.e. M2A, for

15 further comparison with M1B.

Sensitivity analysis indicated that both M1B and M2A were fairly robust, because a ±10% change in each parameter led to less than a 3% change in CVMAE (Fig. 3a and b). When ranges of parameter values obtained from the calibration runs were taken into account (Table 1), the sensitivity to parameter uncertainty became higher for

20 M2A than for M1B (Fig. 3c and d). For M2A, sensitivity to β_2 was much lower than for the other three parameters even if β_2 exhibited a higher CV than the other parameters (Fig. 3d and Table 1).

Two examples of predicted time series using M1B and M2A are shown in Fig. 4. The first example (Fig. 4a) corresponds to a relatively dry site with weak seasonality,

25 while the second shows heavier rainfalls and a more pronounced seasonality (Fig. 4b). Soil moisture dynamics predicted with M2A exhibited more rapid changes and was "peakier" than with M1B. This was particularly the case near the end of the wet season, for example in 2006 at the first site and in 2004 and 2006 in the second site. This impacted the predicted V time series which also showed higher contrasts between dry

and wet periods in M2A compared to M1B. Yearly maximum values of *V* tended to be underestimated by M1B, for example in 2001 and 2006 in the first site and in 2003 and 2004 at the second site. While the timing for leaf onset and leaf offset were correctly predicted by both models, they were less successful in reproducing the multiannual variations in peak amplitude, for example 2003 at the first site and 2002 at the second site.

On a site by site basis, we examined the relationships between model performance and several environmental variables. We found that the magnitude of error (CVMAE) tended to increase with decreasing summer rainfalls for M1B (Fig. 5a) whereas CV-MAE of M2A was much more consistent throughout the rainfall gradient (Fig. 5b). Both models exhibited a significantly higher CVMAE for south-western sites with "brown-red" soils than for northern sites with "grey soils" (data not shown). Because soil type and summer rainfalls covaried in space, it was difficult to tease out the relative impact of these two factors on model performance. There were no relationships between model performance and distance to the nearest rain gauge (Fig. 5c and 5d) and distance to the nearest stock watering point (Fig. 5e and f).

Finally, we explored the ability of both models to predict the integrated value of vegetation cover from July to June. Consistent with model performance reported above (see Table 2), predicted integrated values for M1B were strongly underestimated in the most productive years (slope of SMA=0.66) whereas the magnitude of error for M2A did not change with soil moisture availability (slope of SMA=0.95) (Fig. 6). On the other hand, there were many cases for which M2A incorrectly predicted no peaks when the observations showed small peaks with integrated values <2 (Fig. 6b). As a result, the SMA slope of M2A shifted to the right and the SMA intercept was significantly different from zero (Fig. 6b).

Seasonal leaf dynamics in tropical grasslands

P. Choler et al.

Full Screen / Esc

Printer-friendly Version

Interactive Discussion

4 Discussion

From our exploration of the ability of linear and nonlinear models to predict NDVI-derived vegetation cover in semi-arid perennial grasslands, we conclude that that both types of models had a similar Mean Absolute Error. However, the nonlinear model had the following advantages: (1) it exhibited far less systematic error (Table 2); (2) it had a better ability to capture the sharp transitions in leaf cover, especially under high seasonality of precipitation (Fig. 4); (3) its performance did not deteriorate in the driest sites (Fig. 5a and b); and (4) its parameters are more meaningful because the model aims to capture the fundamental feedbacks between soil and plant growth through a more process-based approach. The main caveat of the nonlinear model was its slightly greater sensitivity to parameter uncertainty (Fig. 3c and d). These points are discussed below.

Most previous studies that have examined relationships between NDVI and climate have done so with linear correlation or regression analyses. Model performance has usually been evaluated using Pearson correlation coefficients (du Plessis, 1999; Wang et al., 2001; Paruelo and Lauenroth, 1998; Chamaille-Jammes et al., 2006; Richard and Poccard, 1998; Wang et al., 2003) although this metric is a poor indicator of goodness-of-fit (Willmott, 1982; Willmott and Matsuura, 2006). In this study, more than two thirds of the NDVI-vegetation cover variability was explained by the linear and nonlinear models (see R-squared values in Table 2) indicating a high responsiveness of these grasslands to soil water balance. Similar values have been reported for other tropical grasslands found on clay soils (Nicholson and Farrar, 1994; Farrar et al., 1994). Our study expands on previous literature because (1) we examined the appropriateness of different model structure to address NDVI-precipitation relationships and (2) we provided a more comprehensive analysis of model performance. In particular, error partitioning indicated that in the case of linear models, no parameter set was able to give unbiased estimates at each time step and along the rainfall gradient (Table 2 and Figs. 4, 6). With a nonlinear model structure the systematic component of the

error was greatly reduced but not the overall uncertainty in model predictions (Table 2). There is no single criteria for a model to be acceptable (Rykiel, 1996) but we advocate that for a given error magnitude it is preferable to retain the model that exhibits the minimum bias.

5   Several studies have focused on the relationships between climate and yearly or seasonally integrated values of NDVI, used as a proxy of productivity (examples in Paruelo and Lauenroth, 1998; Propastin and Kappas, 2008). Such an approach cannot identify fine timing of leaf onset, growth and offset events which are crucial for land surface modelling (Pielke et al., 1998; Dickinson et al., 1998; Bounoua et al., 2006). In

10   the investigated semi-arid tropical grasslands investigated here, the dynamics of leaf cover are characterized by abrupt transitions associated with seasonal water availability (Fig. 4). The amplitude of change in leaf cover in response to soil water content at the start of the growing season was better captured by a nonlinear logistic growth than by the linear model. The same holds for the senescence phase for which the feedback

15   of plant cover on soil moisture was critical to simulate the decline in V. Sharp peaks of leaf biomass in response to resource pulses have long been viewed as archetypal examples of nonequilibrium dynamics (Seastedt and Knapp, 1993; Blair, 1997). The structure of nonlinear models provides much more flexibility to capture these transient maxima. Conversely, finding a common threshold value of W for peak initiation remains

20   a delicate task for nonlinear models, as evidenced by the high coefficient of variation reported for β_5 in M2B (Table 2). Indeed, nonlinearities in M2 naturally tend to exacerbate errors associated with uncertainty in parameters (compare Fig. 3c and d). Nonlinear models did a better job to model peak amplitude and integrated values of plant cover when soil available water was large enough (Figs. 4 and 6), but an unre-

25   solved issue is their tendency to predict more false negatives when seasonal soil water availability was more limited (Fig. 6b).

A key benefit of nonlinear models is that the parameters are more meaningful because they refer to soil water hydrology and ecophysiology of plants. The concept of rain-use efficiency has arisen from a number of studies that examined how precipitation

Seasonal leaf dynamics in tropical grasslands

P. Choler et al.

drives phenology in the tropics (Nicholson and Farrar, 1994). Empirical estimates of rain-use efficiency typically result from applying a low-pass filter to precipitation time-series and then correlating vegetation indices to these smoothed and lagged time-series of predictors. By contrast, a nonlinear modelling framework decomposes rain-use efficiency into different components. For example, it makes explicit the relationship between water extraction by roots (β_2) and plant growth rate (β_3, i.e. the increment of leaf area for a given amount of water extracted from the soil. This opens avenues for linking these phenological models and physiologically-oriented canopy functioning models or biomass allocation models. Hence, nonlinear models offer greater opportunities for coupling with land surface models than their linear counterparts.

There are several reasons why both models fail to explain more NDVI-vegetation cover variability, including (1) observation errors, (2) neglect of other forcing variables and (3) failure of both model structures. As an example of possible observational biases, we found abnormally low NDVI values during the build up phase at the start of the wet season, possibly related to insufficient removal of cloud contamination of the NDVI data. It is likely that predictive models of NDVI time series are more sensitive to this source of errors than models using integrated values during the growing season. Second, there are a number of potential site-specific factors not included in the models that might affect plant phenological response such as contrasting soil water holding capacity, soil fertility, species composition, plant functional diversity, and grazing intensity. It is obviously impossible to translate all these effects into a four parameter model. Our preliminary studies did not provide any evidence for an effect of the distance to the nearest waterpoint, which can be viewed as a surrogate of grazing intensity. Neither did we find that temperature or photoperiod having any significant impact on the leaf dynamics of grasslands in the area covered. Third, the models did not take into account multiannual dynamics. For example, several drought years combined with overgrazing trigger a sharp decline in perennial grasses (Orr, 1980b). Alternatively, two or three consecutive wet years would favour recruitment of new grasses and hence increase the carrying capacity of a given site. Further refinements of the models should be able

to combine short-term and long-term effects of soil water balance. An option would be to add a third state variable representing root storage capacity of carbohydrates.

5 Conclusions

There have been very few attempts to calibrate and validate coupled dynamical sys-
⁵ tems model of soil moisture and plant cover by using time series of remotely sensed data (Seaquist et al., 2003; Hess et al., 1996). Indeed, there is still a gap between em-
pirical, remote-sensing oriented modelling of NDVI-precipitation relationships and more conceptual and theoretical efforts towards process-oriented ecohydrological models (Porporato et al., 2002; Rodriguez-Iturbe et al., 2001). Our study contributed to bridg-
¹⁰ ing this gap by showing that simple nonlinear models of phenology can provide both el-
egant and mechanistic understanding on how precipitation variability affects vegetation growth in semi-arid grasslands. Further work should examine whether this mechanistic framework is also appropriate to modelling phenology at a larger scale, especially for other water-limited ecosystems of the world.

References

²⁰ Archibald, S. and Scholes, R. J.: Leaf green-up in a semi-arid African savanna - separating tree and grass responses to environmental cues, J. Veg. Sci., 18, 583–594, 2007.
Bailey, R. G.: Identifying ecoregion boundaries, Environ. Manag., 34, S14–S26, 2004.
Blair, J. M.: Fire, *N* availability, and plant response in grasslands: A test of the transient maxima hypothesis, Ecology, 78, 2359–2368, 1997.

Seasonal leaf dynamics in tropical grasslands

P. Choler et al.

|◄ | ►|

◄ | ►

Back | Close

Full Screen / Esc

Printer-friendly Version

Interactive Discussion

Botta, A., Viovy, N., Ciais, P., Friedlingstein, P., and Monfray, P.: A global prognostic scheme of leaf onset using satellite data, Glob. Change Biol., 6, 709–725, 2000.

Bounoua, L., Masek, J., and Tourre, Y. M.: Sensitivity of surface climate to land surface parameters: A case study using the simple biosphere model SiB2, J. Geophys. Res. Atmos., 111, D22S09, doi:10.1029/2006JD007309, 2006.

Byrd, R. H., Lu, P. H., Nocedal, J., and Zhu, C. Y.: A Limited Memory Algorithm for Bound Constrained Optimization, Siam J. Sci. Comput., 16, 1190–1208, 1995.

Carlson, T. N., Capehart, W. J., and Gillies, R. R.: A New Look at the Simplified Method for Remote-Sensing of Daily Evapotranspiration, Remote Sens. Environ., 54, 161–167, 1995.

Carlson, T. N. and Ripley, D. A.: On the relation between NDVI, fractional vegetation cover, and leaf area index, Remote Sens. Environ., 62, 241–252, 1997.

Chamaille-Jammes, S., Fritz, H., and Murindagomo, F.: Spatial patterns of the NDVI-rainfall relationship at the seasonal and interannual time scales in an African savanna, Int. J. Remote Sens., 27, 5185–5200, 2006.

Choudhury, B. J., Ahmed, N. U., Idso, S. B., Reginato, R. J., and Daughtry, C. S. T.: Relations between Evaporation Coefficients and Vegetation Indexes Studied by Model Simulations, Remote Sens. Environ., 50, 1–17, 1994.

Christie, E. K.: Biomass and Nutrient Dynamics in a C-4 Semi-Arid Australian Grassland Community, J. Appl. Ecol., 18, 907–918, 1981.

Chuine, I.: A unified model for budburst of trees, J. Theor. Biol., 207, 337–347, 2000.

Churkina, G. and Running, S. W.: Contrasting climatic controls on the estimated productivity of global terrestrial biomes, Ecosystems, 1, 206–215, 1998.

Daly, E. and Porporato, A.: A review of soil moisture dynamics: From rainfall infiltration to ecosystem response, Environ. Eng. Sci., 22, 9–24, 2005.

De Michele, C., Vezzoli, R., Pavlopoulos, H., and Scholes, R. J.: A minimal model of soil water-vegetation interactions forced by stochastic rainfall in water-limited ecosystems, Ecol. Model., 212, 397–407, 2008.

Dickinson, R. E., Shaikh, M., Bryant, R., and Graumlich, L.: Interactive canopies for a climate model, J. Climate, 11, 2823–2836, 1998.

Dickinson, R. E., Tian, Y. H., Liu, Q., and Zhou, L. M.: Dynamics of leaf area for climate and weather models, J. Geophys. Res.-Atmos., 113, D16115, 2008.

du Plessis, W. P.: Linear regression relationships between NDVI, vegetation and rainfall in Etosha National Park, Namibia, J. Arid Environ., 42, 235–260, 1999.

Seasonal leaf dynamics in tropical grasslands

P. Choler et al.

Farrar, T. J., Nicholson, S. E., and Lare, A. R.: The Influence of Soil Type on the Relationships between Ndvi, Rainfall, and Soil-Moisture in Semiarid Botswana. 2. Ndvi Response to Soil-Moisture, Remote Sens. Environ., 50, 121–133, 1994.

Foran, B. D. and Bastin, G.: The dynamics of a Mitchell grass (*Astrebla* spp.) rangeland on the Barkly Tableland, Northern Territory, Aust. Rangeland J., 6, 92–97, 1984.

Gutman, G. and Ignatov, A.: The derivation of the green vegetation fraction from NOAA/AVHRR data for use in numerical weather prediction models, Int. J. Remote Sens., 19, 1533–1543, 1998.

Hess, T., Stephens, W., and Thomas, G.: Modelling NDVI from decadal rainfall data in the North East Arid Zone of Nigeria, J. Environ. Manag., 48, 249–261, 1996.

Huxman, T. E., Smith, M. D., Fay, P. A., Knapp, A. K., Shaw, M. R., Loik, M. E., Smith, S. D., Tissue, D. T., Zak, J. C., Weltzin, J. F., Pockman, W. T., Sala, O. E., Haddad, B. M., Harte, J., Koch, G. W., Schwinning, S., Small, E. E., and Williams, D. G.: Convergence across biomes to a common rain-use efficiency, Nature, 429, 651–654, 2004.

Jeffrey, S. J., Carter, J. O., Moodie, K. B., and Beswick, A. R.: Using spatial interpolation to construct a comprehensive archive of Australian climate data, Environ. Model. Softw., 16, 309–330, 2001.

Ji, L. and Peters, A. J.: A spatial regression procedure for evaluating the relationship between AVHRR-NDVI and climate in the northern Great Plains, Int. J. Remote Sens., 25, 297–311, 2004.

Lotsch, A., Friedl, M. A., Anderson, B. T., and Tucker, C. J.: Coupled vegetation-precipitation variability observed from satellite and climate records, Geophys. Res. Lett., 30, 1774, doi:1710.1029/2003GL017506, 2003.

McKenzie, N. J. and Hook, J.: Interpretation of the Atlas of Australian Soils, CISRO, Canberra, ACT, Australia, 61 pp., 1992.

McKenzie, N. J., Jacquier, D. W., Ashton, L. J., and Cresswell, H. P.: Estimation of soil properties using the Atlas of Australian Soils, CSIRO, Canberra, ACT, Australia, 24, 2000.

Mebane W. R. and Sekhon J. S.: R-GENetic Optimization Using Derivatives (RGENOUD), online available at: http://sekhon.berkeley.edu/rgenoud/, 2009.

Montandon, L. M. and Small, E. E.: The impact of soil reflectance on the quantification of the green vegetation fraction from NDVI, Remote Sens. Environ., 112, 1835–1845, 2008.

Myneni, R. B., Hall, F. G., Sellers, P. J., and Marshak, A. L.: The Interpretation of Spectral Vegetation Indexes, IEEE T. Geosci. Remote, 33, 481–486, 1995.

Nicholson, S. E. and Farrar, T. J.: The Influence of Soil Type on the Relationships between Ndvi, Rainfall, and Soil-Moisture in Semiarid Botswana. 1. Ndvi Response to Rainfall, Remote Sens. Environ., 50, 107–120, 1994.

Orr, D. M.: A review of *Astrebla* (Mitchell Grass) pastures in Australia, Trop. Grassl., 9, 21–36, 1975.

Orr, D. M.: Effects of Sheep Grazing *Astrebla* Grassland in Central Western Queensland. 1. Effects of Grazing Pressure and Livestock Distribution, Aust. J. Agr. Res., 31, 797–806, 1980a.

Orr, D. M.: Effects of Sheep Grazing *Astrebla* Grassland in Central Western Queensland, J. Aust. Inst. Agr. Sci., 46, 185–185, 1980b.

Paruelo, J. M. and Lauenroth, W. K.: Interannual variability of NDVI and its relationship to climate for North American shrublands and grasslands, J. Biogeogr., 25, 721–733, 1998.

Pettorelli, N., Vik, J. O., Mysterud, A., Gaillard, J. M., Tucker, C. J., and Stenseth, N. C.: Using the satellite-derived NDVI to assess ecological responses to environmental change, Trends Ecol. Evol., 20, 503–510, 2005.

Pickup, G., Bastin, G. N., and Chewings, V. H.: Identifying trends in land degradation in non-equilibrium rangelands, J. Appl. Ecol., 35, 365–377, 1998.

Pielke, R. A., Avissar, R., Raupach, M., Dolman, A. J., Zeng, X. B., and Denning, A. S.: Interactions between the atmosphere and terrestrial ecosystems: influence on weather and climate, Glob. Change Biol., 4, 461–475, 1998.

Porporato, A., D'Odorico, P., Laio, F., Ridolfi, L., and Rodriguez-Iturbe, I.: Ecohydrology of water-controlled ecosystems, Adv. Water Res., 25, 1335–1348, 2002.

Potter, C. S. and Brooks, V.: Global analysis of empirical relations between annual climate and seasonality of NDVI, Int. J. Remote Sens., 19, 2921–2948, 1998.

Priestley, C. H. B. and Taylor, R. J.: Assessment of Surface Heat-Flux and Evaporation Using Large-Scale Parameters, Mon. Weather Rev., 100, 81–92, 1972.

Propastin, P. A. and Kappas, M.: Reducing uncertainty in modeling the NDVI-precipitation relationship: A comparative study using global and local regression techniques, Gisci. Remote Sens., 45, 47–67, 2008.

Raupach, M. R.: Dynamics of resource production and utilisation in two-component biosphere-human and terrestrial carbon systems, Hydrol. Earth Syst. Sci., 11, 875–889, 2007, http://www.hydrol-earth-syst-sci.net/11/875/2007/.

Raupach, M. R., Briggs, P. R., Haverd, V., King, E. A., Paget, M., and Trudinger, C. M.: Aus-

Seasonal leaf dynamics in tropical grasslands

P. Choler et al.

Title Page

Abstract	Introduction
Conclusions	References
Tables	Figures

◀◀ ▶▶

◀ ▶

Back Close

Full Screen / Esc

Printer-friendly Version

Interactive Discussion

tralian Water Availability Project (AWAP). Final report for Phase 3, CISRO, Canberra, ACT, Australia, 61 pp., 2008.

Richard, Y. and Poccard, I.: A statistical study of NDVI sensitivity to seasonal and interannual rainfall variations in Southern Africa, Int. J. Remote Sens., 19, 2907–2920, 1998.

5 Rodriguez-Iturbe, I., Porporato, A., Laio, F., and Ridolfi, L.: Plants in water-controlled ecosystems: active role in hydrologic processes and response to water stress – I. Scope and general outline, Adv. Water Res., 24, 695–705, 2001.

Rykiel, E. J.: Testing ecological models: The meaning of validation, Ecol. Model., 90, 229–244, 1996.

10 Savitzky, A. and Golay, M. J. E.: Smoothing and Differentiation of Data by Simplified Least Squares Procedures, Anal. Chem., 36, 1627–1639, 1964.

Seaquist, J. W., Olsson, L., and Ardo, J.: A remote sensing-based primary production model for grassland biomes, Ecol. Model., 169, 131–155, 2003.

Seastedt, T. R. and Knapp, A. K.: Consequences of Nonequilibrium Resource Availability

15 across Multiple Time Scales – the Transient Maxima Hypothesis, Am. Nat., 141, 621–633, 1993.

Walker, B. H. and Langridge, J. L.: Modelling plant and soil water dynamics in semi-arid ecosystems with limited site data, Ecol. Model., 87, 153–167, 1996.

Wang, J., Price, K. P., and Rich, P. M.: Spatial patterns of NDVI in response to precipitation and

20 temperature in the central Great Plains, Int. J. Remote Sens., 22, 3827–3844, 2001.

Wang, J., Rich, P. M., and Price, K. P.: Temporal responses of NDVI to precipitation and temperature in the central Great Plains, USA, Int. J. Remote Sens., 24, 2345–2364, 2003.

Willmott, C. J.: Some comments on the evaluation of model performance, Bull. Am. Meteorol. Soc., 63, 1309–1313, 1982.

25 Willmott, C. J. and Matsuura, K.: On the use of dimensioned measures of error to evaluate the performance of spatial interpolators, Int. J. Geo. Inform. Sci., 20, 89–102, 2006.

Seasonal leaf dynamics in tropical grasslands

P. Choler et al.

Full Screen / Esc

6, 8661–8690, 2009

Seasonal leaf dynamics in tropical grasslands

P. Choler et al.

Title Page

Abstract | Introduction

Conclusions | References

Tables | Figures

|◄ | ►|

◄ | ►

Back | Close

Full Screen / Esc

Printer-friendly Version

Interactive Discussion

Table 1. Calibrated values of parameters for linear (M1) and nonlinear (M2) models (see Eqs. 2 and 3). Mean (± se) and coefficient of variation (CV) were calculated from 30 calibration runs each using 100 randomly sampled calibrating sites. The mean values of the objective function, i.e. the median of CVMAE (see Eq. 4), are also indicated.

Model	Statistics	Objective Function (CVMAE)	α_1	$\alpha_2 \times 10^4$	α_3		
M1A	Mean (± se)	0.77 (± 0.0021)	3.88 (± 0.05)	7.64 (± 0.14)			
	CV (%)	1.5	7.7	10.2			
M1B	Mean (± se)	0.65 (± 0.0027)	1.97 (± 0.06)	13.73 (± 0.46)	71.58 (± 2.97)		
	CV (%)	1.7	11.9	13.7	17.1		
Model	Statistics	Objective Function (CVMAE)	β_1	β_2	β_3	β_4	β_5
M2A	Mean (± se)	0.67 (± 0.0038)	6.17 (± 0.24)	0.48 (± 0.03)	12.14 (± 0.48)	0.6 (± 0.03)	
	CV (%)	2.3	16.2	23.5	16.2	19.7	
M2B	Mean (± se)	0.65 (± 0.0019)	5.24 (± 0.18)	0.63 (± 0.02)	12.04 (± 0.27)	0.53 (± 0.02)	9.79 (± 1.39)
	CV (%)	1.6	18.7	18.3	12.1	19.6	76.7

Table 2. Compared performance of linear (M1) and nonlinear (M2) models (see Eqs. 2 and 3). After each of the 30 calibration runs, goodness-of-fit statistics were calculated for the 300 remaining testing sites. Therefore, reported values are the means of 30×300 estimates. n is the number of time steps.

	M1A	M1B	M2A	M2B
n	368	368	368	368
r^2	0.68	0.73	0.70	0.71
MAE	0.034	0.028	0.029	0.029
CVMAE	0.839	0.673	0.678	0.681
RMSE	0.071	0.060	0.064	0.064
CVRMSE	1.721	1.537	1.589	1.591
Systematic error (%)	86.1	55.3	32.1	29.1
Unsystematic error (%)	13.9	44.7	67.9	70.9
Elevation (SMA)	0.0093	−0.0005	−0.0068	−0.0078
$P_{(H0:elevation=0)}$	0.03	0.24	0.26	0.23
Slope (SMA)	0.47	0.77	0.86	0.89
$P_{(H0:slope=1)}$	0.006	0.053	0.106	0.109

Printer-friendly Version

Interactive Discussion
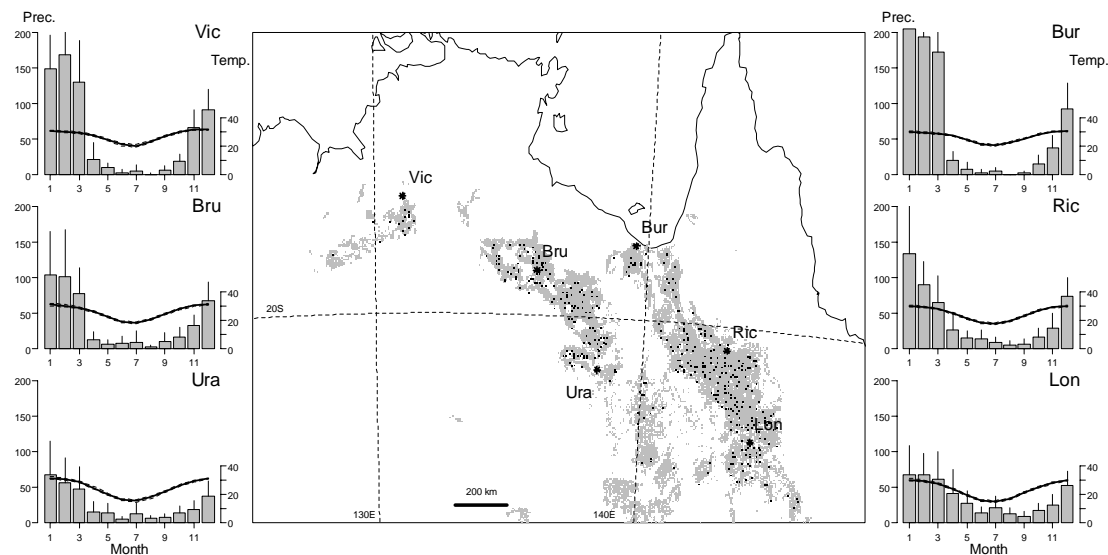
Fig. 1. Geographical distribution of Mitchell grasslands (grey) and location of the 400 random sites investigated. Left and right panels show monthly means (+ 1 sd) of precipitation (mm) and mean temperature (°C) over the period 1961–1990 as recorded in 8 weather stations within or nearby the Mitchell grasslands area. Abbreviations are as follows: Bru: Brunette Downs; Bur: Burketown; Ric: Richmond; Ura: Urandangi; Vic: Victoria Rivers. Map projection is Albers Equal Area Conic projection.

Seasonal leaf dynamics in tropical grasslands

P. Choler et al.
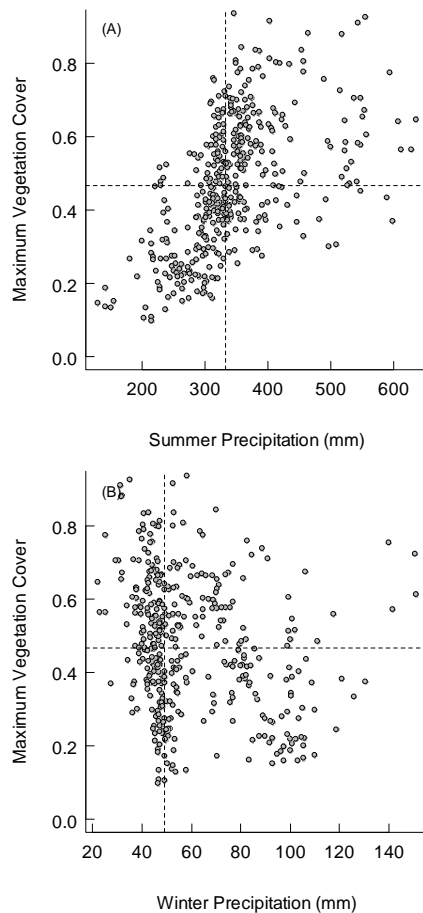
Fig. 2. Relationship between the maximum vegetation cover (K) over the period 2000–2008 and the mean "summer", i.e. from November to April **(A)** and the mean "winter", i.e. from May to October **(B)** precipitation. Each point represents one of the 400 random sites investigated. Dotted lines represent median values.
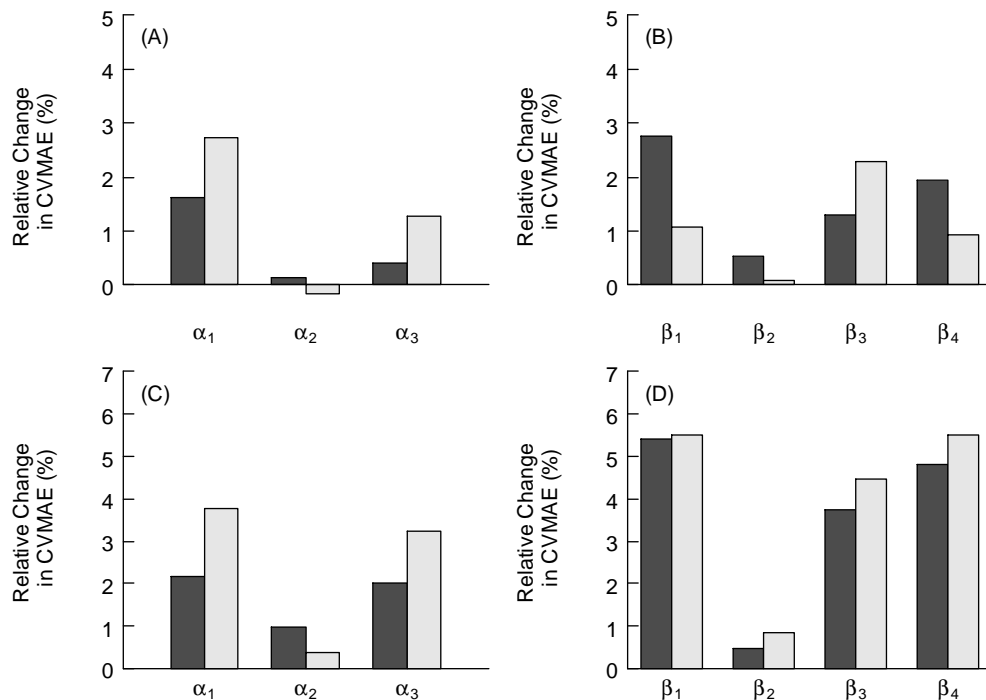
Fig. 3. Robustness of M1B **(A, C)** and M2A **(B, D)** to parameter uncertainty. Histograms show the effect of an increase (grey) and a decrease (black) of a parameter on the relative change of CVMAE. Magnitude of the change is ± 10% (A, B) and ±CV (C, D) where CV is the coefficient of variation resulting from the calibration runs (see Table 1).
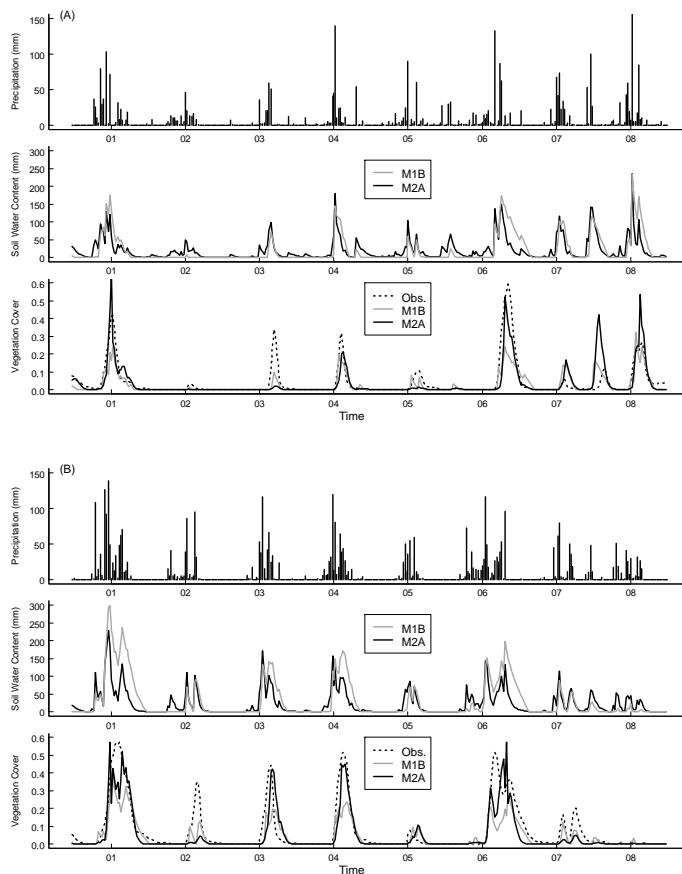
Fig. 4. Example of two 8 yr time series of rainfalls and predicted soil water content (W in mm) and vegetation cover (V) for a relatively dry site **(A)** and a wetter site **B)**. Dotted lines are for observed time series of V. Plain lines represent predicted values with M1B (gray) and M2A (black).
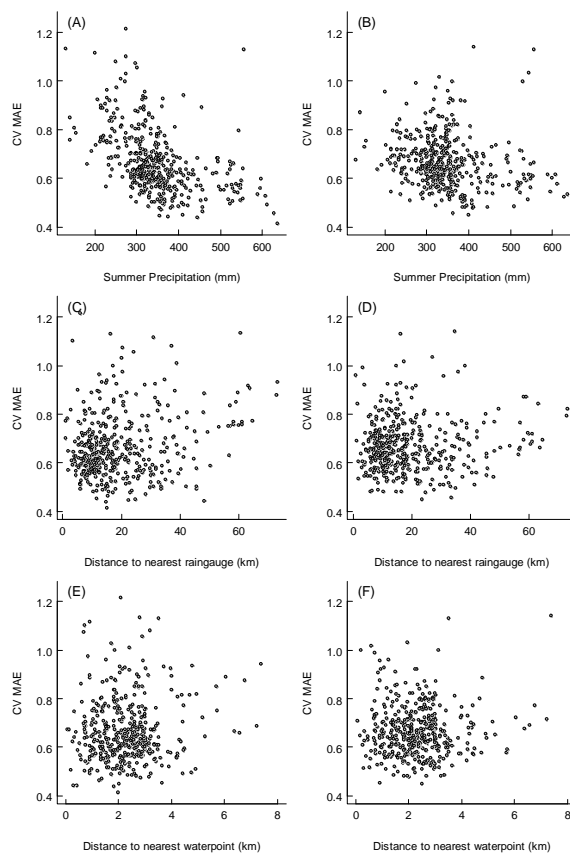
Fig. 5. Effect of summer precipitation **(A, B)**, distance to the nearest rain gauge **(C, D)** and distance to the nearest stock waterpoint **(E, F)** on model performance estimated by CVMAE. For each of the 400 sites, predicted values were calculated with model M1B (A, C, E) and model M2A (B, D, F) using parameter values of Table 1.
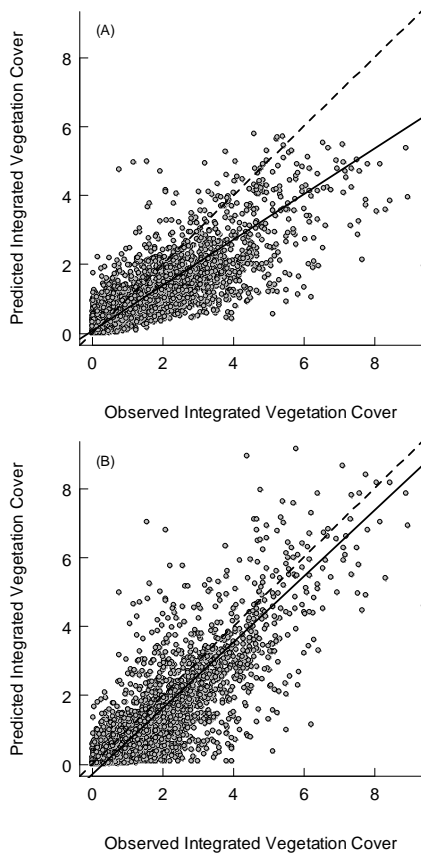
Fig. 6. Observed *vs.* predicted values of yearly integrated vegetation cover with model M1B **(A)** and model M2A **(B)**. Each point represents one site for one year. Dotted lines show the 1:1 relationship and plain lines show the Standardized Major Axes (SMA).